(2)

ARMY RESEARCH LABORATORY

AD-A260 784

Computation of the Roll Moment Coefficient for a Projectile With Wrap-Around Fins

Harris L. Edge

ARL-TR-23 December 1992

NOTICES

Destroy this report when it is no longer needed. DO NOT return it to the originator.

Additional copies of this report may be obtained from the National Technical Information Service, U.S. Department of Commerce, 5285 Port Royal Road, Springfield, VA 22161.

The findings of this report are not to be construed as an official Department of the Army position, unless so designated by other authorized documents.

The use of trade names or manufacturers' names in this report does not constitute indorsement of any commercial product.

DISCLAIMER NOTICE

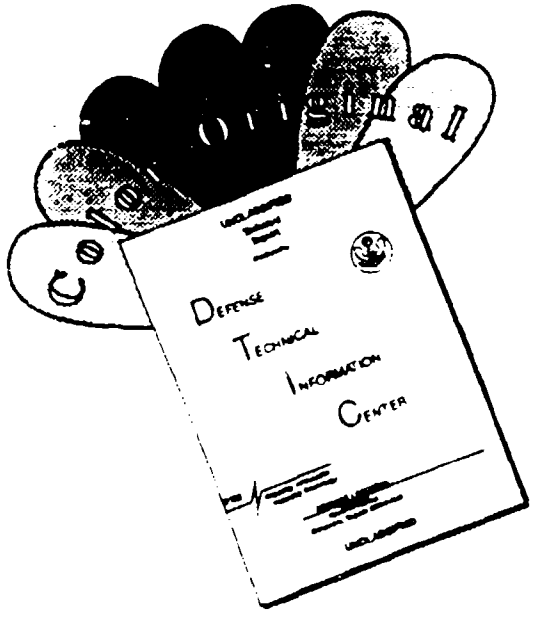

THIS DOCUMENT IS BEST QUALITY AVAILABLE. THE COPY FURNISHED TO DTIC CONTAINED A SIGNIFICANT NUMBER OF COLOR PAGES WHICH DO NOT REPRODUCE LEGIBLY ON BLACK AND WHITE MICROFICHE.

REPORT DOCUMENTATION PAGE

Form Approved
OMB No. 0704-0188

1. AGENCY USE ONLY (Leave blank)	2. REPORT DATE	3. REPORT TYPE AND DATES COVERED
	December 1992	Final, December 1990 - January 1992

4. TITLE AND SUBTITLE

COMPUTATION OF THE ROLL MOMENT COEFFICIENT FOR A PROJECTILE WITH WRAP-AROUND FINS

5. FUNDING NUMBERS

1L161102AH43

6. AUTHOR(S)

HARRIS L. EDGE

7. PERFORMING ORGANIZATION NAME(S) AND ADDRESS(ES)

8. PERFORMING ORGANIZATION REPORT NUMBER

9. SPONSORING / MONITORING AGENCY NAME(S) AND ADDRESS(ES)

US Army Research Laboratory
ATTN: AMSRL-OP-CI-B (Tech Lib)
Aberdeen Proving Ground, Maryland 21005-5066

10. SPONSORING / MONITORING AGENCY REPORT NUMBER

ARL-TR-23

11. SUPPLEMENTARY NOTES

The report supersedes BRL-IMR-969, October 1991.

12a. DISTRIBUTION / AVAILABILITY STATEMENT

Approved for public release; distribution is unlimited.

12b. DISTRIBUTION CODE

13. ABSTRACT (Maximum 200 words)

Flow field solutions of a projectile with wrap-around fins have been computed for velocities ranging from Mach 1.3 to Mach 3. The flow field solutions were computed with a time-marching, 3-D, zonal, full Navier-Stokes code. The roll moment coefficient was computed from the flow field solutions and compared to the roll moment coefficient obtained experimentally for a similar wrap-around fin projectile. The roll moment coefficient computations show favorable agreement with experimental measurements in predicting changes of the roll moment coefficient magnitude and sign as a function of the flight Mach number. This demonstrates computational fluid dynamics' capability as a promising method for reliably predicting the roll moment coefficient of projectiles with wrap-around fins.

14. SUBJECT TERMS		15. NUMBER OF PAGES
Aerodynamics Aerodynamic Stability Computations Fin Stabilized Ammunition	Fluid Dynamics Folding Fins Tube Launched	24 16. PRICE CODE

17. SECURITY CLASSIFICATION OF REPORT	18. SECURITY CLASSIFICATION OF THIS PAGE	19. SECURITY CLASSIFICATION OF ABSTRACT	20. LIMITATION OF ABSTRACT
UNCLASSIFIED	UNCLASSIFIED	UNCLASSIFIED	UL

INTENTIONALLY LEFT BLANK.

Acknowledgment

The author would like to thank the members of the Computational Aerodynamics Branch and Dr. N. Patel for giving their support, advice, and technical expertise. The advice of the reviewers, Dr. W. Sturek and Dr. P. Plostins, was greatly appreciated.

INTENTIONALLY LEFT BLANK.

TABLE OF CONTENTS

INTENTIONALLY LEFT BLANK.

LIST OF FIGURES

INTENTIONALLY LEFT BLANK.

1. INTRODUCTION

Wrap-around fins have been used primarily for their advantages in packaging tube-launched projectiles. The wrap-around fin conforms to the cylindrical shape of the projectile while in the launch tube, allowing more efficient use of space. Thus, greater numbers of wrap-around fin projectiles can be stored in the same space as fixed-fin projectiles designed to deliver the same payload (Dahlke 1975; Winchenbach 1986).

The cylindrical shape of the wrap-around fin is advantageous for packaging; but it can also be compromising to the dynamic stability of the projectile. In many configurations that wrap-around fins have been employed, it has been noted that the roll moment coefficient may change in magnitude and sign as the Mach number varies (Dahlke 1975; Winchenbach 1986,Mermagen 1981). During the course of flight of a wrap-around fin projectile, it is possible for its spin rate to increase or decrease more than once. In addition, the direction of spin may change. This type of behavior can produce poor flight dynamics. In order to design dynamically stable projectiles employing wrap-around fins, it is necessary to have the ability to predict the roll moment coefficient at all flight conditions for the full trajectory. Design code methodology is inadequate for this problem (Dahlke 1990). Results from computational fluid dynamics (CFD) calculations have shown promise. Normal force coefficients calculated using inviscid CFD computations have compared favorably with experimental data. However, roll moment coefficients calculated using inviscid CFD computations have not shown good agreement with experimental data (Wardlaw 1987). This paper presents the initial results for establishing the capability of predicting the roll moment coefficient for a projectile with wrap-around fins through viscous computations with a 3-D full Navier-Stokes code.

2. ABOUT THE TEST CASE

The experimental data used for comparison were obtained from references 1, 6 and 7. The reports document a comprehensive effort to experimentally determine how changes in geometry affect the aerodynamic forces generated by wrap-around fins. A standard wrap-around fin projectile determined by the Technical Cooperation Program (TTCP), as seen in Figure 1, was used as the basic configuration. A number of geometric variations to the basic configuration were made. The aerodynamic forces of each configuration were measured and documented. The configuration for the wrap-around fin projectile modeled in the computation was derived from the standard set by the TTCP (Dahlke 1975, Dahlke 1976). Although the body retains the dimensions of the standard TTCP configuration, the fins differ slightly. The standard TTCP configuration had fins with symmetric leading and

trailing edge bevels. The computational model had blunt leading and trailing edges. There is a difference of 45 degrees between the root and tip chord in the standard TTCP configuration while the root and tip chord are parallel in the computational model. See Figures 2 and 4 for a visual reference. Another difference to note is that the standard TTCP configuration had boundary layer trips on the body and the fin leading edges (Dahlke 1975, Dahlke 1976). The boundary layer was laminar for the body and fins for the computational model.

Flowfield solutions were computed for a series of Mach numbers ranging from 1.3 to 3.0 at sea-level atmospheric conditions. The freestream conditions were: density = $1.198 kg/m^3$; static temperature = $21.6^0 C$; and static pressure = $101.3 kPa$. The Reynolds number, based on projectile length, for sea-level conditions ranged from 30 to 69 million. Flowfield solutions were also computed using wind tunnel free stream conditions. The Reynolds number under wind tunnel conditions varied from 17 million at Mach 1.3 to 69 million at Mach 3.0. The wind tunnel atmospheric conditions were obtained from reference 7. The experimental data were obtained from four different sites: the McDonnell Douglas Aerophysics wind tunnel; the Arnold Engineering Development Center (AEDC); NASA Langley Research Center; and the Jet Propulsion Laboratory (JPL). The experiments conducted by McDonnell Douglas, AEDC and NASA Langley were wind tunnel tests while the JPL data were obtained from a free flight test (Dahlke 1975, Dahlke 1976). The models used in the McDonnell Douglas, AEDC and NASA Langley experiments followed the TTCP specifications. The models used to obtain the experimental data at JPL were scaled versions of those used for the wind tunnel experiments. These models did not have boundary layer trips on the leading edges of the fins (Dahlke 1975, Dahlke 1976). The experimentally obtained roll moment coefficients have been compared to values computed from flowfield solutions calculated by the BRL ZONAL Navier-Stokes code. Wind tunnel data were available comparing the TTCP standard configuration with a configuration that had blunt leading and trailing edges. See Figure 3 for this configuration. These data will be discussed later.

3. CODE AND BOUNDARY CONDITIONS

All flowfield solutions were computed with the BRL Zonal code. The BRL Zonal code is a 3-D full Navier-Stokes code which can be applied to zonal grid topologies. The governing equations are numerically integrated by an explicit time-marching method (Patel, Sturek and Smith 1989; Patel and Edge 1991).

The flowfield solutions were viscous flow calculations. The computationally modeled surface was one-fourth of the entire projectile surface. The symmetry of the projectile allowed the modeling of one fin and approximately forty-five degrees of body surface on either side

of the fin. A periodic boundary condition was written to take advantage of this symmetry. This helped to reduce the number of grid cells needed for the computation, but it restricted the angle of attack to zero degrees. The calculation of the roll moment coefficient was the primary goal in this initial effort. For this reason, the flowfield was computed for the body and fins only, since the influence of the recirculating flow at the base on the roll moment coefficient is expected to be small. Future computations which include flow field solutions at the projectile base will hopefully verify the accuracy of this assumption. A zero gradient boundary condition was used at the trailing edges of the fins for the downstream boundary condition. A non-reflecting boundary condition was applied to the outermost grid plane from the body surface. The non-reflecting boundary condition allowed the outermost grid plane to be placed relatively close to the body, which reduced the number of computational points needed for a solution. In order to obtain a viscous solution, the fin and body surfaces were modeled with a no-slip boundary condition.

A zonal approach was used to obtain a solution for the flowfield. In the zonal approach, as implemented in the BRL Zonal code, overlapped zones share at least one grid cell in a given direction with an adjacent zone. The shared grid cells have identical coordinates in both of the overlapped zones. Since the two overlapped zones have the same coordinates for the shared grid cells, zonal coupling requires only the transfer of information from the field of one zone to the boundary of the other zone and vice-versa. No interpolation is required. A multi-zone solution is obtained by performing the integration of the governing equations in all zones and then exchanging information between overlapping zones before advancing to the next iteration (Patel, Sturek and Smith 1989; Patel and Edge 1991).

All computations were performed on a Cray-2 supercomputer. Some flowfield solutions were computed on the TACOM Cray-2 while others were computed on the Cray-2 at BRL. As configured for this case, the BRL Zonal code required forty-five million words of memory.

4. GRID

The zonal approach facilitated the building of the computational grid. The unswept wrap-around fins with blunt leading edges would have been difficult to model with a wrap-around grid. The use of a wrap-around grid would have resulted in large and rapid variations of the metric terms, which could have severely degraded the quality of the solution (Patel, Sturek and Smith 1989; Patel and Edge 1991). The zonal approach allowed the accurate modelling of the wrap-around fin projectile's geometry while retaining a smooth continuous computational mesh. A cut-away view of the computational grid can be seen in Figure 5.

The grid was designed for viscous computation. It was highly clustered near the body and fin surfaces. The total number of points used for the computation was 951,888. The dimensions for each of the seven zones were as follows, (20 x 80 x 32), (20 x 80 x 32), (130 x 80 x 32), (130 x 80 x 32), (20 x 80 x 18), (96 x 80 x 18), (36 x 26 x 48). As stated earlier, these seven zones were configured to model one-fourth of the wrap-around fin projectile.

An algebraic grid generator, developed at BRL, was used to build the computational mesh. Once the interior mesh of a zone is completed, grid points on the boundary are added, deleted or changed to create overlaps between adjacent zones. In order for the periodic boundary condition to function properly, the planes in which data were exchanged were spaced such that they were exactly ninety degrees apart in the circumferential direction.

5. RESULTS

Qualitatively, the flowfield solutions computed by the BRL Zonal code show a number of interesting features of wrap-around fin aerodynamics. Figures 6, 7 and 8 show surface pressure contours on the concave and convex sides of the wrap-around fins at different Mach numbers. These figures show the influence of shocks generated at the fin leading edge on the fin surface. In addition, the figures also show the development of a high pressure region near the leading edge of the concave side of the fin as the Mach number increases.

The differences in the surface pressure contours on the convex and concave sides of the fin are quite evident. Figure 9 is a view of the wrap-around fin from its concave side. Figure 10 is a view from the convex side. Figure 11 shows a view between the fins. Near the fin root, the shock generated by the fin is clearly asymmetric. Figure 12 shows a flowfield plane away from the body that intersects the fin at approximately fifty percent of its height. It should be noted that the plane is not at a constant radial distance from the body surface. The shock on the concave and convex sides of the fin appear to be very similar to each other at a distance away from the body. Near the fin leading edge at the root of the fin, the surface pressure on the concave and convex sides of the fin appear to be very different from each other.

Figure 13 shows the flowfield at various axial stations along the fin length. These contours give a good indication of the overall structure of shocks generated by a wrap-around fin projectile. The contours also show the "focusing" of the shock on the concave side of the fin. This is most apparent near the leading edge of the fin. Generally speaking, the leading edge is the area where there is the greatest difference in pressure between the concave and convex sides of the fin. This is in agreement with the findings mentioned in Reference 1.

A comparison of the computed roll moment coefficient and the experimentally obtained roll moment coefficient shows good agreement with overall trends. Figure 14 is a graph showing the roll moment coefficient versus Mach number for experimental data obtained at JPL and computations made from the BRL Zonal code solutions. Figure 14 shows that the roll moment coefficients computed from BRL Zonal code flowfield solutions follow the general trends of the experimental data. At lower Mach numbers, the roll moment coefficient is positive. At higher Mach numbers, the roll moment coefficient is negative. A positive roll moment coefficient indicates a roll direction towards the fin's center of curvature. The predicted and JPL measured roll moment coefficients indicate one cross-over point, a Mach number at which the roll moment coefficient is zero, near Mach 1.7 .

It is expected that the geometrical differences between the computational model and the TTCP standard configuration would produce differences in their roll moment coefficients. Additional wind tunnel data are presented to show how the fin bluntness affects the roll moment coefficient. Figure 15 is a roll moment coefficient versus Mach number plot for two wrap-around fin configurations obtained under similar conditions. One configuration is the standard TTCP configuration while the second configuration is a modified TTCP configuration which has blunt fin edges. Figure 3 shows the fin geometry of this second configuration. The data are presented because the fin leading edge bluntness is the primary geometrical difference between the TTCP standard configuration and the computational model. As can be seen in Figure 15, the roll moment coefficient versus Mach number curve of the blunt finned configuration seems to retain the same overall characteristics of the curve for the TTCP standard configuration. The differences in the two curves indicate that a blunt leading edge as opposed to a forty-five degree leading edge wrap-around fin will have a slightly higher cross-over point and, subsonically at least, have a greater roll moment coefficient.

A comparison of the different roll moment coefficients of a standard TTCP configuration obtained from various facilities shows some scatter in the data, but the overall trends stated earlier, remain intact. Figure 16 is a plot of roll moment coefficient versus Mach number for experimental data obtained using the TTCP standard configuration. As stated earlier, the McDonnell Douglas, AEDC and Langley data were obtained from wind tunnel experiments with the standard TTCP configuration. The JPL free-flight data were obtained using a scaled down version of the TTCP standard configuration. The model used at JPL did not have boundary layer trips on the fin leading edges while the models used at McDonnell Douglas, AEDC and Langley did have fin leading edge boundary layer trips (Dahlke 1975, Dahlke 1976). In the Dahlke 1975 and 1976 reports, the data in Figure 16 was presented with a discussion of the effects of Reynolds number on roll moment coefficient. The experimental

data indicate that the Reynolds number may have an effect on the roll moment coefficient and Dahlke speculated the Reynolds number and the lack of boundary layer trips may be responsible for the difference in the JPL data and the other experimental data. The JPL data predicts the cross-over point to be at approximately Mach 1.7 while the other wind tunnel data indicates Mach 1. With the exception of the differing cross-over points, the JPL data agrees well with the other wind tunnel data. The computed roll moment coefficients, shown in Figure 14, indicate that there is little difference in the roll moment coefficient under wind tunnel, (Reynolds number 17 to 23 million) and sea-level, (Reynolds numbers 30 to 69 million) conditions.

6. CONCLUDING REMARKS

Flowfield solutions of a wrap-around fin projectile were calculated with the BRL 3-D Zonal Navier-Stokes code. The roll moment coefficient was calculated from the flowfield solutions and compared to the roll moment coefficient obtained from experiment measurements for a similar wrap-around fin projectile configuration. The computed roll moment coefficients predicted the same trends seen in the experimentally obtained roll moment coefficients in magnitude and sign, (direction). Experimental data obtained from McDonnell Douglas, AEDC and NASA Langley wind tunnels indicated that the cross-over point was at Mach 1 while the JPL free flight data indicated that the cross-over point was greater than Mach 1. It is encouraging that the computed roll moment coefficient cross-over point was close to the cross-over point of the JPL free flight data. The boundary layer was laminar on the fins in the computational model. Also, the model used for the JPL experiments did not have a boundary layer trip on the fin leading edge, while the models used in the wind tunnel experiments did. Another point to note is that the JPL experiments had the lowest Reynolds number. This raises the possibility that the wrap-around fins of the JPL model may have had a laminar boundary layer at low Mach numbers which would give this experiment another feature in common with the computation. The experimental data indicate that the roll moment coefficient varies with the Reynolds number. However, the data do not establish any trends which would allow one to state conclusively whether there is a relationship between the Reynolds number and roll moment coefficient or what that relationship may be. The results from the CFD computations do not indicate that the roll moment coefficient is Reynolds number dependent.

The roll moment coefficient computations have shown good agreement, in terms of the magnitude and sign, with values of the roll moment coefficient obtained experimentally. The computational technique, as outlined in this report, has shown great promise in being a

reliable method for predicting the roll moment coefficient. However, a one-to-one comparison of computation and experiment is difficult to make. As this is an ongoing effort, further work will be done to fully establish this capability. Future plans include: 1) applying the F3D code to wrap-around fin configurations (Sahu 1988); 2) computing turbulent viscous flowfield solutions; and 3) computing flowfield solutions for small angles of attack.

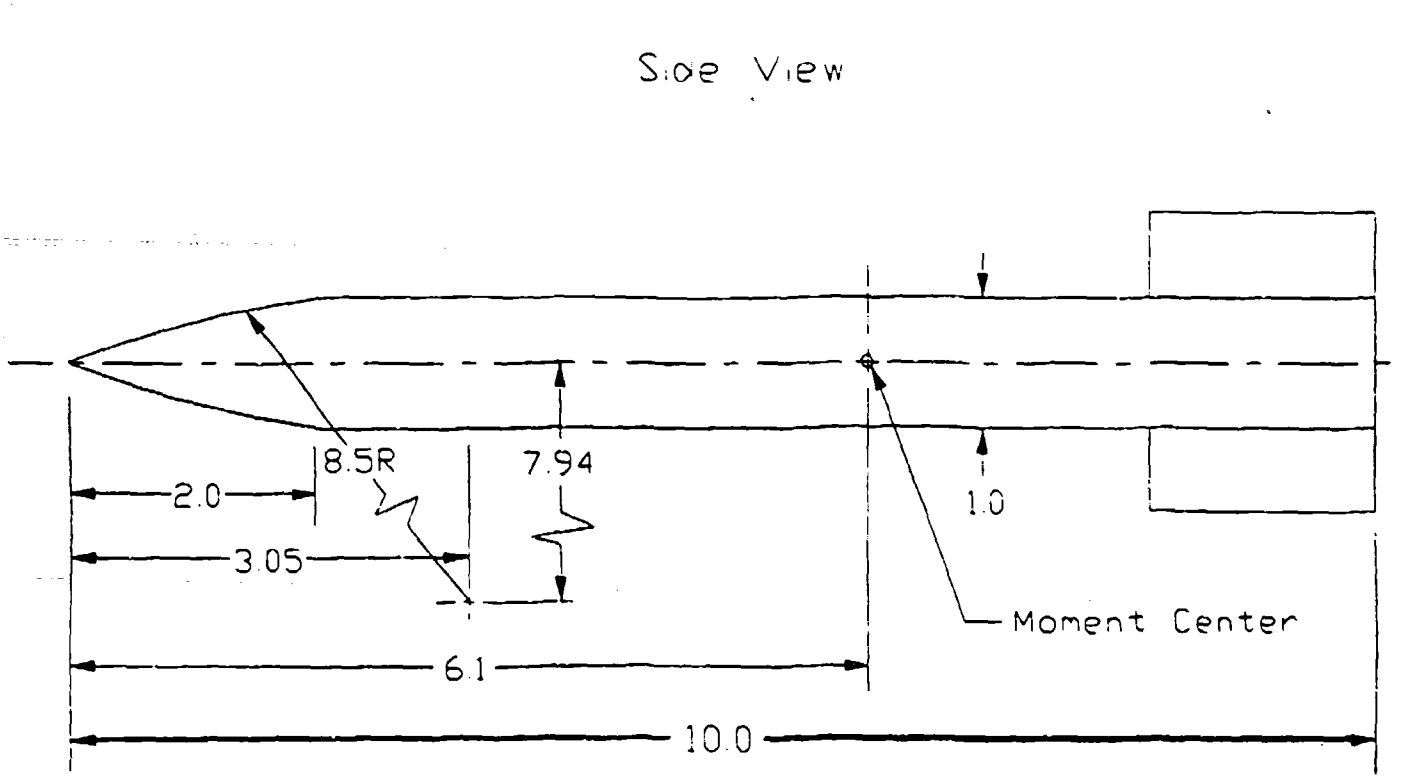

Figure 1. Wrap-around Fin Model Geometry

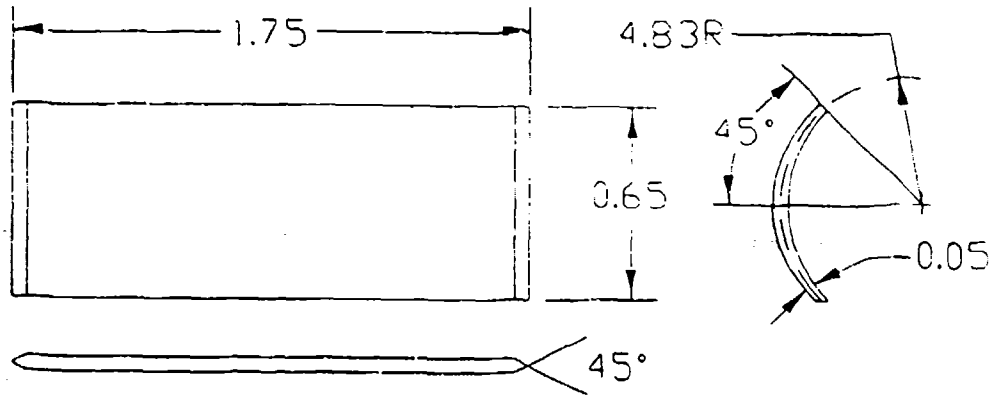

Figure 2. TTCP Standard Wrap-around Fin

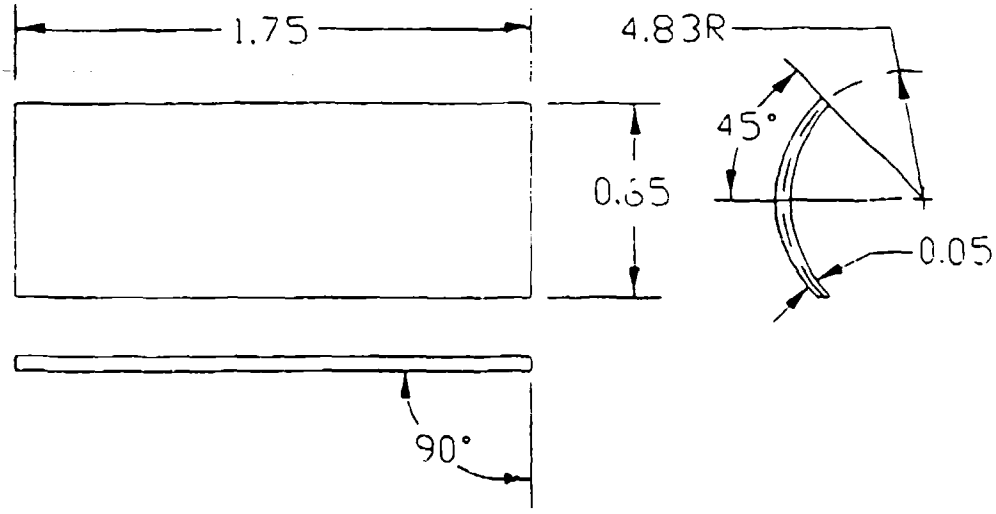

Figure 3. Blunt Leading Edge Wrap-around Fin

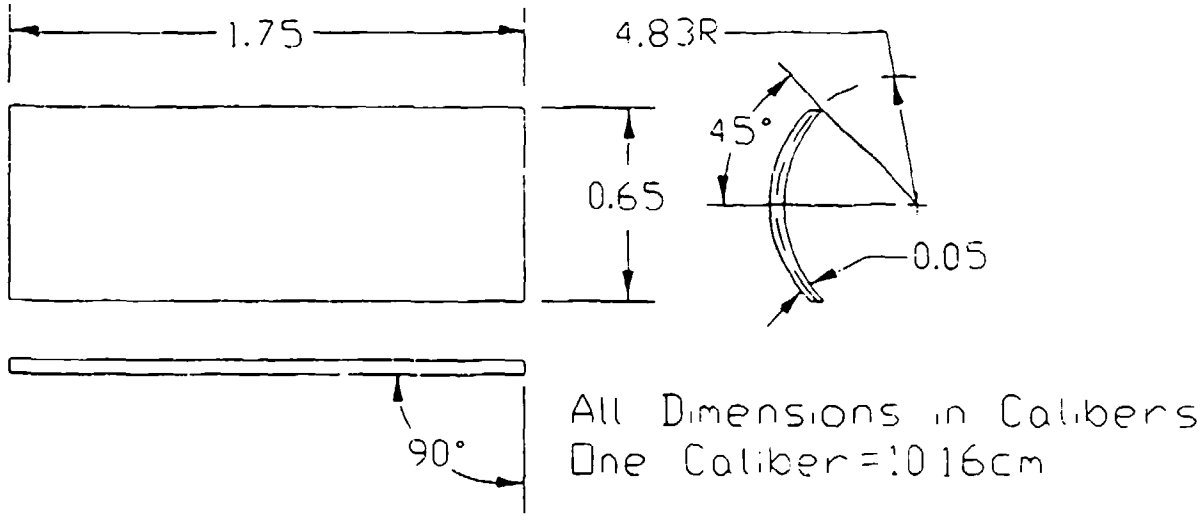

Figure 4. Computational Model Wrap-around Fin

Following page intentionally left blank

Figure 5. Computational Grid

Following page intentionaliy left blank

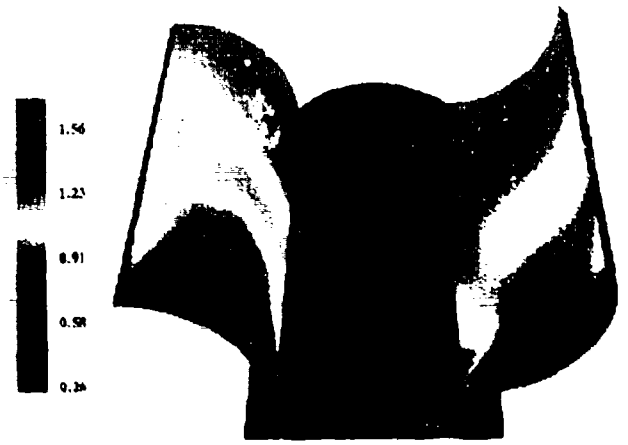

Figure 6. Normalized Pressure Contours at Mach=1.5

Figure 7. Normalized Pressure Contours at Mach=2.0

Figure 8. Normalized Pressure Contours at Mach=2.5

Following page intentionally left blank

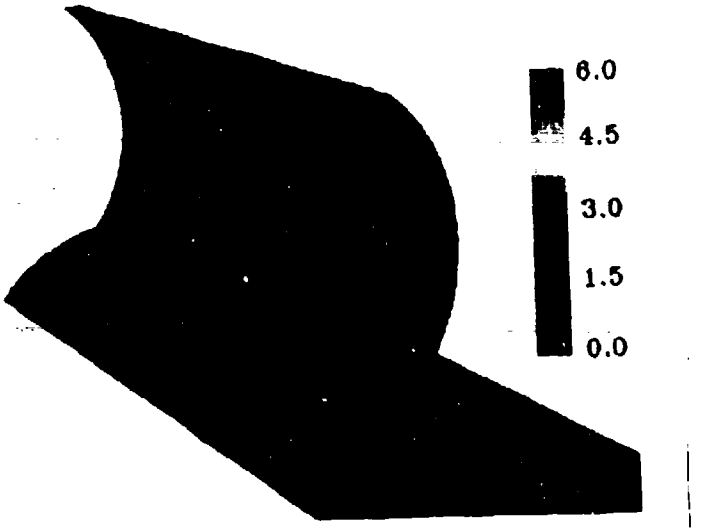

Figure 9. Normalized Pressure Contours on Concave Side of Fin at Mach=2

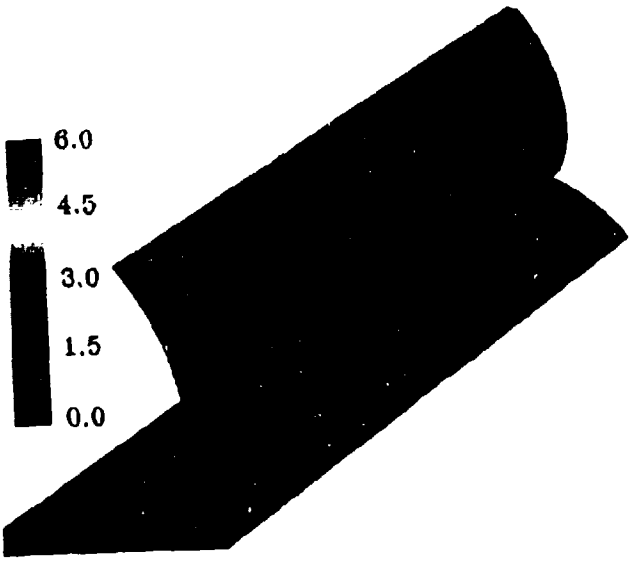

Figure 10. Normalized Pressure Contours on Convex Side of Fin at Mach=2

Following page intentionally left blank

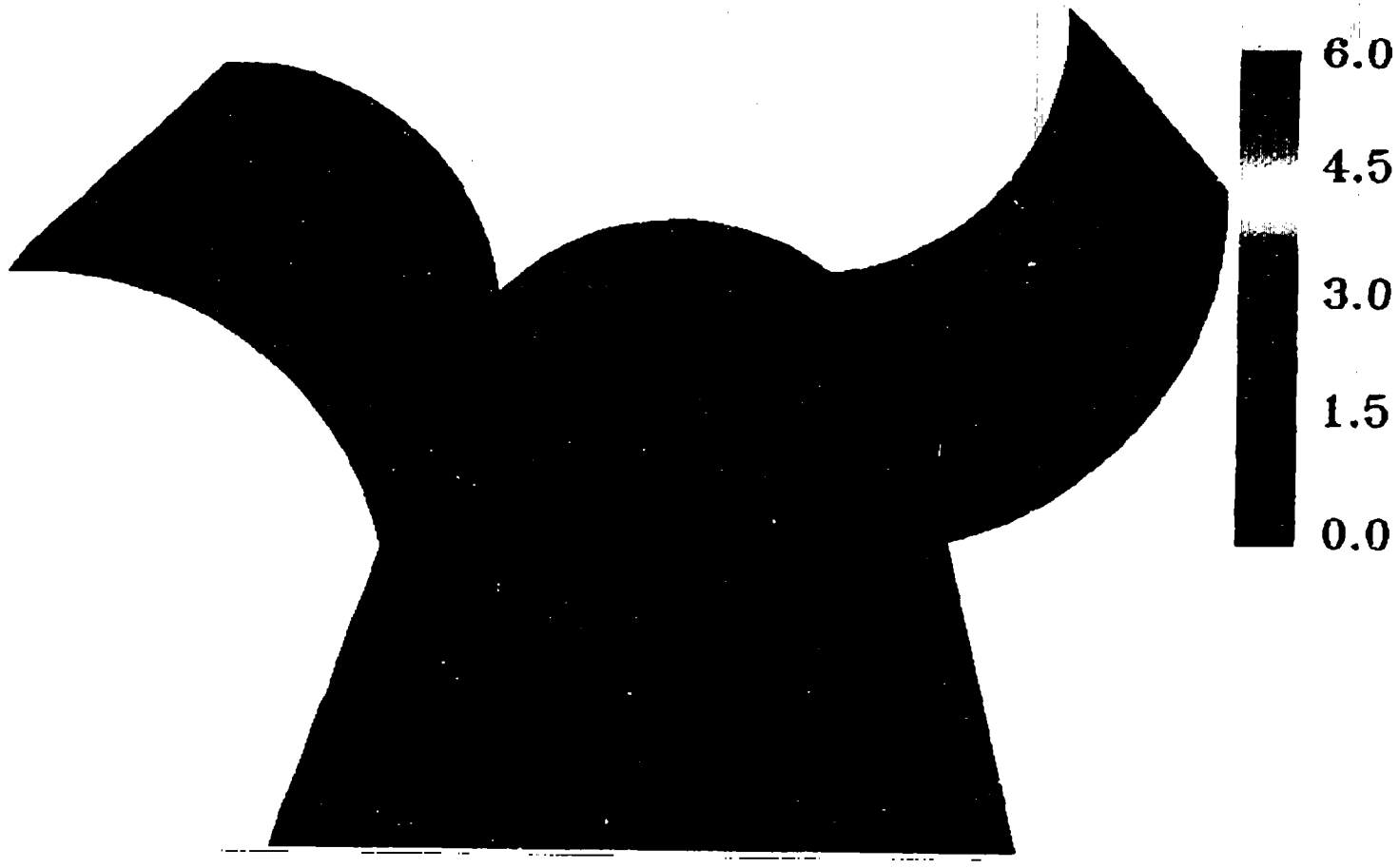

Figure 11. Normalized Pressure Contours Between Fins at Mach=2

Following page intentionally left blank

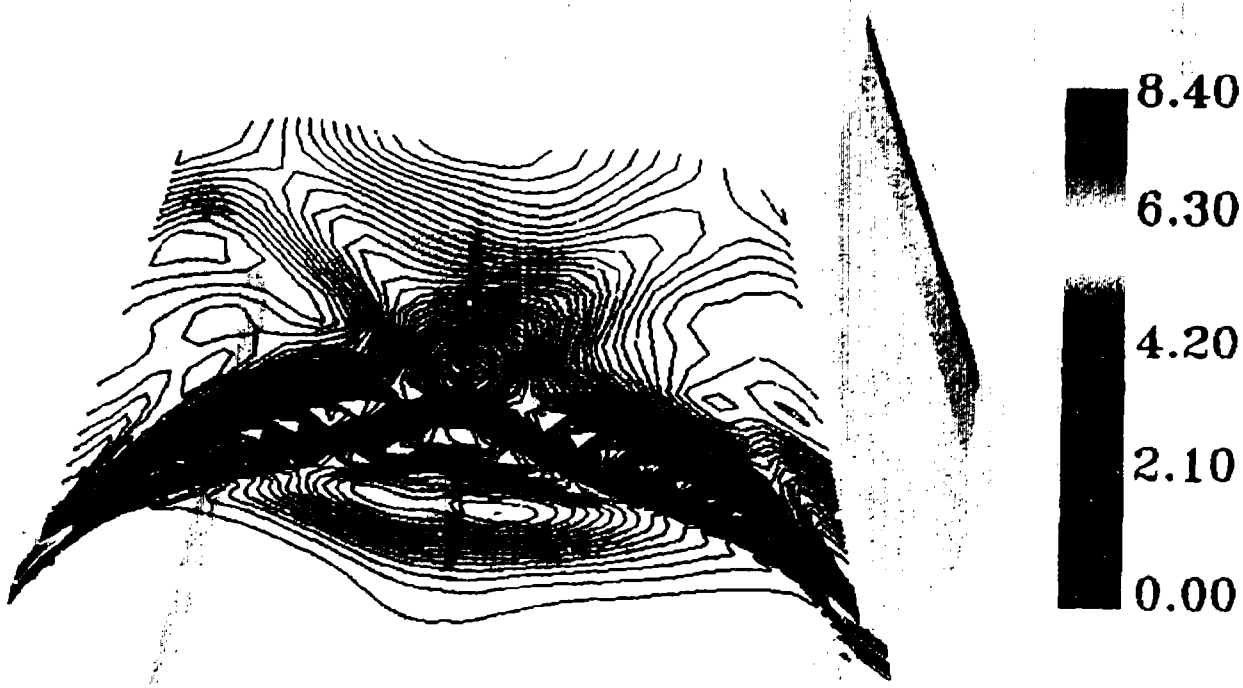

Figure 12. Normalized Pressure Contours Between Fins at Mach=2.5

Following page intentionally left blank

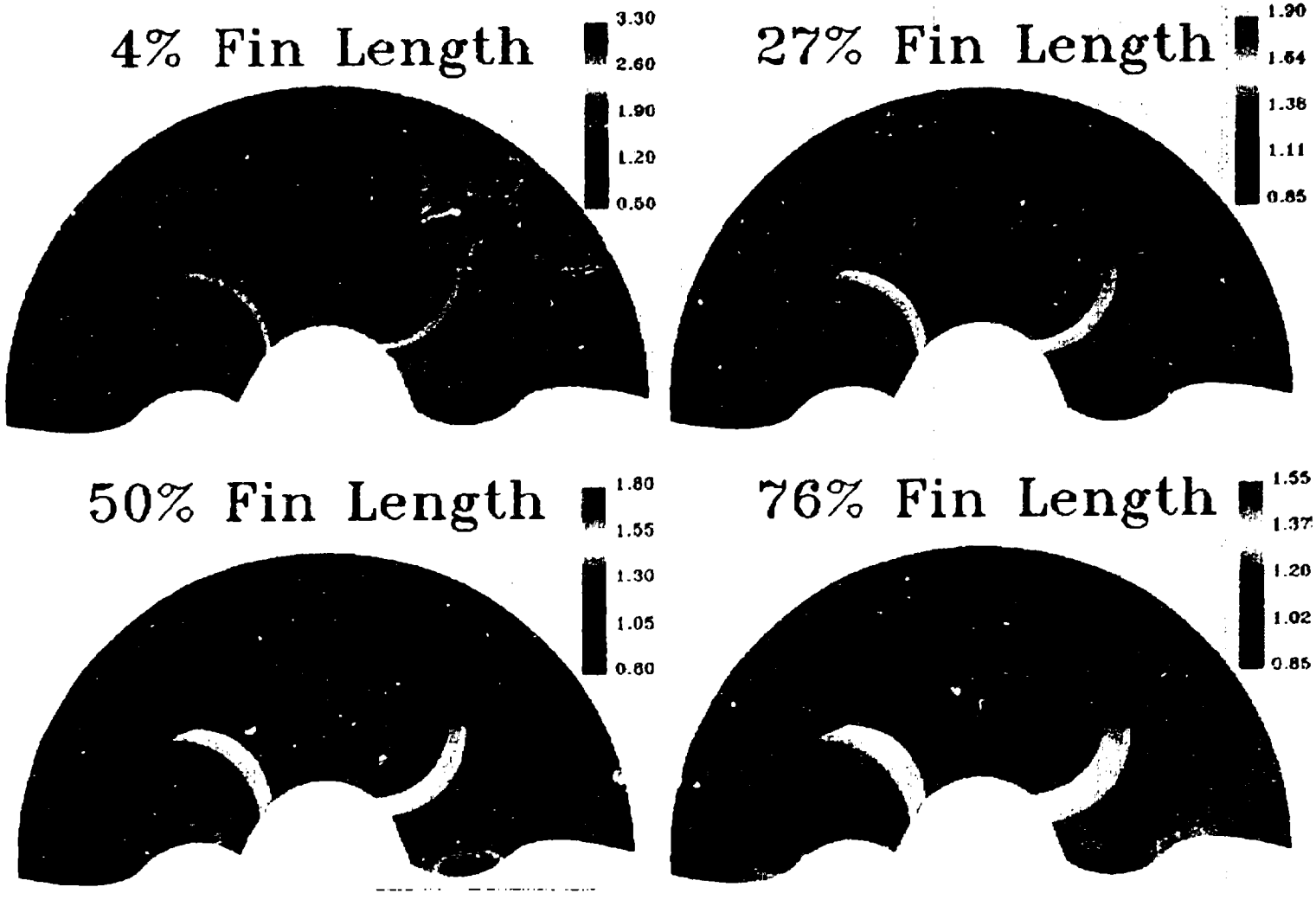

Figure 13. Normalized Pressure Contours at Various Axial Stations at Mach=2.5

Following page intentionally left blank

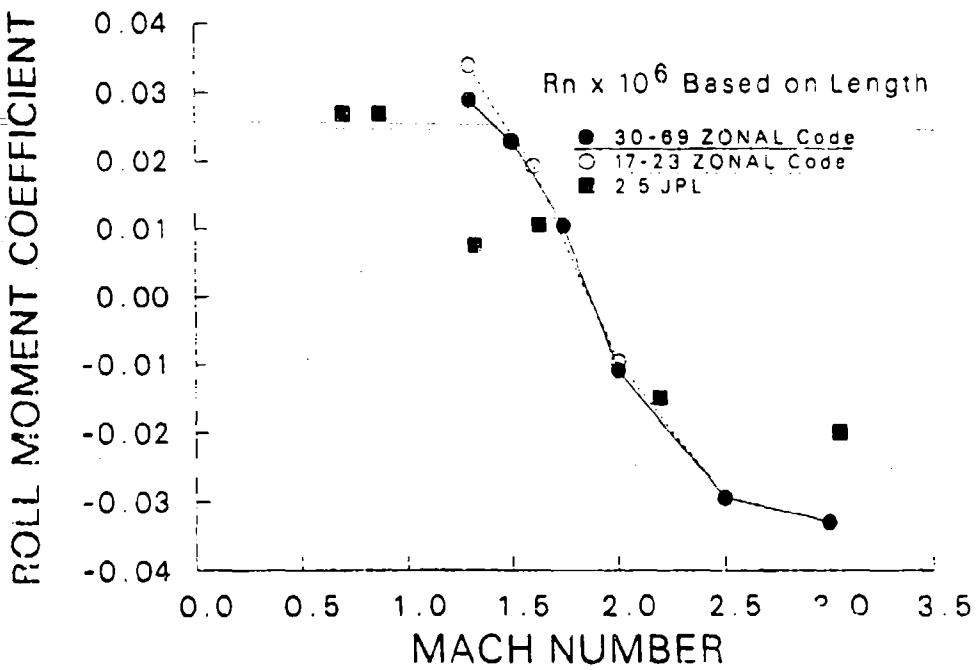

Figure 14. Roll Moment Coefficient vs. Mach Number for Computational and JPL Experimental Data.

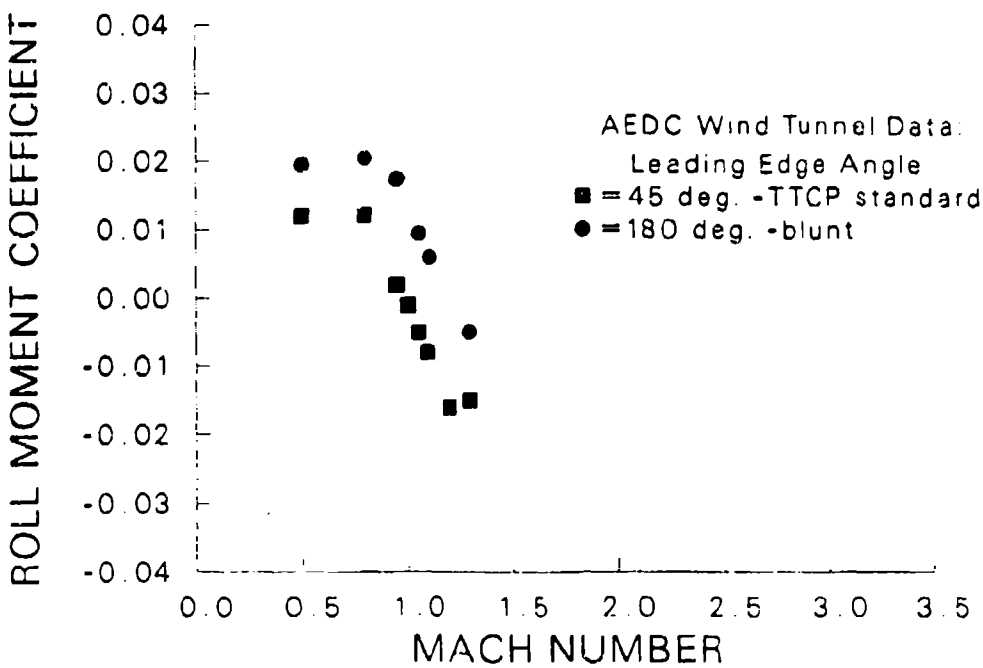

Figure 15. Roll Moment Coefficient vs. Mach Number for Configurations With Different Leading Edge Bluntness.

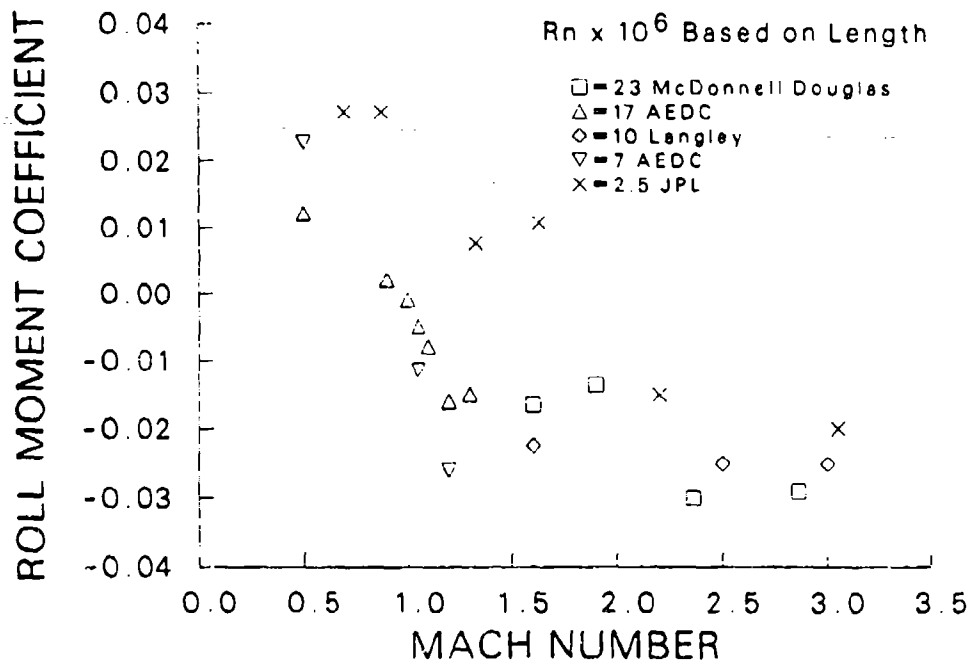

Figure 16. Roll Moment Coefficient vs. Mach Number for Experimental Data.

7. REFERENCES

Dahlke, C. W. "A Review and Status of Wrap-Around Fin Aerodynamics." Tenth Navy Symposium on Aeroballistics, vol. 1, no. 10, pp. 279-324, Naval Surface Weapons Center, Dahlgren Laboratory, Dahlgren, VA, July 1975.

Dahlke, C. W. "The Aerodynamic Characteristcs of Wrap-Around Fins at Mach Numbers of 0.3 to 3.0." Technical Report RD-77-4, U.S. Army Missile Command, Redstone Arsenal, AL, October 1976.

Dahlke, C. W. and G. Batiuk. "Hydra 70 MK66 Aerodynamics and Roll Analysis." Technical Report RD-SS-90-6, U.S. Army Missile Command, Redstone Arsenal, AL, July 1990.

Humphery, J. A., and C. W. Dahlke. "A Summary of Aerodynamic Characteristics for Wrap Around Fins from Mach 0.3 to 3.0" Technical Report TD-77-5, U.S. Army Missile Command, Redstone Arsenal, AL, March 1977.

Mermagen, W. H. and V. Oskay. "Yawsonde Tests of 2.75-Inch Mk66 Mod 1 Rocket." ARBRL-MR-03127, U.S. Army Ballistic Research Laboratory, Aberdeen Proving Ground, MD, August 1981.

Patel, N. R., W. B. Sturek, and G. A. Smith. "Parallel Computation of Supersonic Flows Using a Three-dimensional, Zonal, Navier-Stokes Code." BRL-TR-3049, U.S. Army Ballistic Research Laboratory, Aberdeen Proving Ground, MD, November 1989.

Patel, N. R. and H. L. Edge. "Computations of Integrated Inlet-Combustor Flows for National Aerospace Plane Engine." BRL-IMR-3049, U.S. Army Ballistic Research Laboratory, Aberdeen Proving Ground, MD, February 1991.

Sahu, J. "Numerical Computations of Transonic Critical Aerodynamic Behavior." BRL-TR-2962, U.S. Army Ballistic Research Laboratory, Aberdeen Proving Ground, MD, December 1988.

Wardlaw, A. B., F. J. Priolo, and J. M. Solomon. "Multiple-Zone Strategy for Supersonic Missiles." Journal of Spacecraft and Rockets, vol. 24, no. 4, pp. 377-84, July-August 1987.

Winchenbach, G. L., R. S. Buff, R. H. Whyte, and W. H. Hathaway. "Subsonic and Transonic Aerodynamics of a Wraparound Fin Configuration." Journal of Guidance and Control, vol. 9, no. 6, pp. 627-32, November-December 1986.

INTENTIONALLY LEFT BLANK.

No. of Copies	Organization
2	Administrator Defense Technical Info Center ATTN: DTIC-DDA Cameron Station Alexandria, VA 22304-6145
1	Commander U.S. Army Materiel Command ATTN: AMCAM 5001 Eisenhower Ave. Alexandria, VA 22333-0001
1	Director U.S. Army Research Laboratory ATTN: AMSRL-D 2800 Powder Mill Rd. Adelphi, MD 20783-1145
1	Director U.S. Army Research Laboratory ATTN: AMSRL-OP-CI-AD, Tech Publishing 2800 Powder Mill Rd. Adelphi, MD 20783-1145
2	Commander U.S. Army Armament Research, Development, and Engineering Center ATTN: SMCAR-IMI-I Picatinny Arsenal, NJ 07806-5000
2	Commander U.S. Army Armament Research, Development, and Engineering Center ATTN: SMCAR-TDC Picatinny Arsenal, NJ 07806-5000
1	Director Benet Weapons Laboratory U.S. Army Armament Research, Development, and Engineering Center ATTN: SMCAR-CCB-TL Watervliet, NY 12189-4050
(Unclass. only) 1	Commander U.S. Army Rock Island Arsenal ATTN: SMCRI-IMC-RT/Technical Library Rock Island, IL 61299-5000
1	Director U.S. Army Aviation Research and Technology Activity ATTN: SAVRT-R (Library) M/S 219-3 Ames Research Center Moffett Field, CA 94035-1000

No. of Copies	Organization
1	Commander U.S. Army Missile Command ATTN: AMSMI-RD-CS-R (DOC) Redstone Arsenal, AL 35898-5010
1	Commander U.S. Army Tank-Automotive Command ATTN: ASQNC-TAC-DIT (Technical Information Center) Warren, MI 48397-5000
1	Director U.S. Army TRADOC Analysis Command ATTN: ATRC-WSR White Sands Missile Range, NM 88002-5502
1	Commandant U.S. Army Field Artillery School ATTN: ATSF-CSI Ft. Sill, OK 73503-5000
(Class. only) 1	Commandant U.S. Army Infantry School ATTN: ATSH-CD (Security Mgr.) Fort Benning, GA 31905-5660
(Unclass. only) 1	Commandant U.S. Army Infantry School ATTN: ATSH-CD-CSO-OR Fort Benning, GA 31905-5660
1	WL/MNOI Eglin AFB, FL 32542-5000
	Aberdeen Proving Ground
2	Dir, USAMSAA ATTN: AMXSY-D AMXSY-MP, H. Cohen
1	Cdr, USATECOM ATTN: AMSTE-TC
1	Dir, ERDEC ATTN: SCBRD-RT
1	Cdr, CBDA ATTN: AMSCB-CI
1	Dir, USARL ATTN: AMSRL-SL-I
10	Dir, USARL ATTN: AMSRL-OP-CI-B (Tech Lib)

No. of Copies	Organization
5	Commander U.S. Army Armament Research, Development & Engineering Center ATTN: SMCAR-AET R. Kline H. Hudgins J. Grau S. Kahn M. Siclari Picatinny Arsenal, NJ 07806-5001
3	Commander Air Force Armament Laboratory ATTN: AFATL/FXA B. Simpson G. Abate R. Adelgren Eglin AFB, FL 32542-5434
2	Alliant Techsystems, Inc. Mail Station MN48-3700 7225 Northland Dr. ATTN: Armament Systems Division M. Swenson R. Burretta Brooklyn Park, MN 55428

USER EVALUATION SHEET/CHANGE OF ADDRESS

This Laboratory undertakes a continuing effort to improve the quality of the reports it publishes. Your comments/answers to the items/questions below will aid us in our efforts.

1. ARL Report Number ARL-TR-23 Date of Report December 1992

2. Date Report Received _____

3. Does this report satisfy a need? (Comment on purpose, related project, or other area of interest for which the report will be used.) _____

4. Specifically, how is the report being used? (Information source, design data, procedure, source of ideas, etc.) _____

5. Has the information in this report led to any quantitative savings as far as man-hours or dollars saved, operating costs avoided, or efficiencies achieved, etc? If so, please elaborate. _____

6. General Comments. What do you think should be changed to improve future reports? (Indicate changes to organization, technical content, format, etc.) _____

CURRENT ADDRESS

_____
Organization

_____
Name

_____
Street or P.O. Box No.

_____
City, State, Zip Code

7. If indicating a Change of Address or Address Correction, please provide the Current or Correct address above and the Old or Incorrect address below.

OLD ADDRESS

_____
Organization

_____
Name

_____
Street or P.O. Box No.

_____
City, State, Zip Code

(Remove this sheet, fold as indicated, staple or tape closed, and mail.)

DEPARTMENT OF THE ARMY

OFFICIAL BUSINESS

BUSINESS REPLY MAIL
FIRST CLASS PERMIT No 0001, APG, MD

Postage will be paid by addressee

Director
U.S. Army Research Laboratory
ATTN: AMSRL-OP-CI-B (Tech Lib)
Aberdeen Proving Ground, MD 21005-5066

NO POSTAGE
NECESSARY
IF MAILED
IN THE
UNITED STATES